

Structure and Stoichiometry Self-Organization in a Mixed Vanadium-Iron Oxide Honeycomb Film on Ru(0001)

Piotr Igor Wemhoff^a, Claudine Noguera^b, Jacek Goniakowski^{b*}, and Niklas Nilus^{a*}

^a Carl von Ossietzky Universität Oldenburg, Institut für Physik, D-26111 Oldenburg, Germany

^b CNRS-Sorbonne Université, Institut des Nanosciences de Paris, UMR 7588, F-75005 Paris, France

1. STM conductance spectroscopy – Electronic structure

The different structural elements of the mixed honeycomb oxide can be distinguished not only in topographic but also in differential conductance (dI/dV) maps taken as a function of bias voltage (Fig. S1). The boundary lines separating the regular (2×2) domains produce low contrast in dI/dV maps taken at negative polarity, which points to a low DOS of the O ions in the dislocation network. At positive bias, the regular, defect-free (2×2) regions develop highest dI/dV contrast at ~ 1.0 V, and the domain boundaries are not detectable anymore. Also, the different point defects are readily identified in the maps. At small negative bias, especially type I defects stick out due to their strongly reduced conductance signal, while type II defects exhibit a similar contrast as the regular domains. At positive polarity, the type II defects increase their conductance above the level of regular (2×2) patches around E_F , but turn dark at ~ 0.5 V. Only beyond 2.0 V, their dI/dV contrast increases again, following a similar behavior as observed in the topographic channel. Apparently, this defect type develops an effective tunneling channel at ~ 3.0 V sample bias. The type I defects, on the other hand, exhibit reduced dI/dV intensity throughout the entire bias window explored here (Fig. S1).

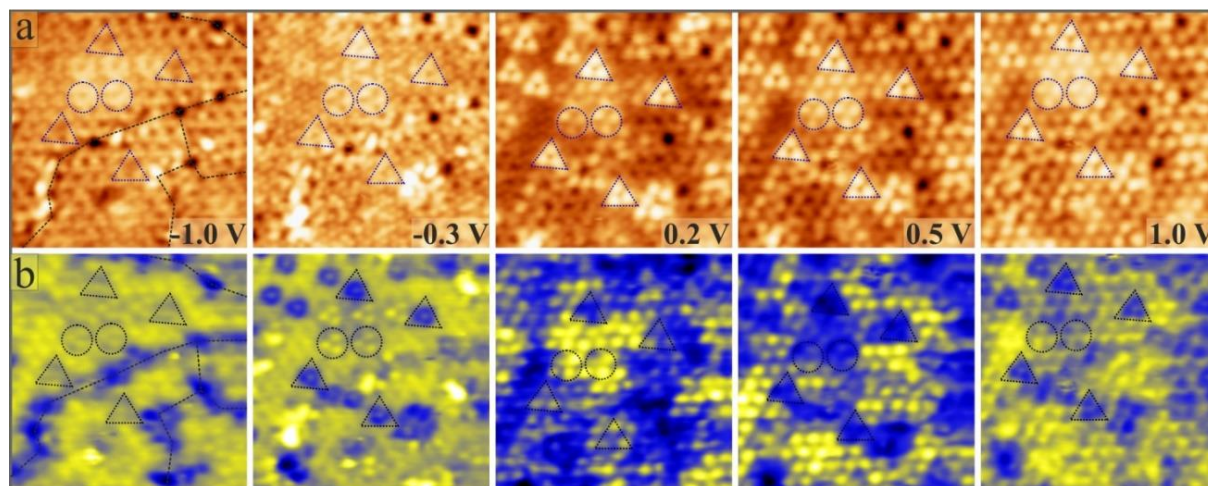


Figure S1: (a) STM topography and (b) dI/dV maps of the V/Fe mixed honeycomb oxide on Ru(0001) probed at the indicated bias voltage (8×8 nm², $I = 1.0$ nA). Examples for type I and type II defects are marked with triangles and circles, respectively. Grain boundaries in the oxide film are shown by dashed lines.

2. XPS - Chemical composition

Insights into the chemical state of mixed honeycomb lattices on Ru(0001) were obtained with XPS, performed with an Al $k\alpha$ source and a detector aligned with the surface normal. The evaluation of the

XPS peaks in Fe 2p, V 2p and O 1s energy windows was done by Shirley background subtraction followed by Gaussian fitting. The O 1s maximum was fixed at 530 eV, in correspondence to respective literature values for FeO(111) bilayers on Ru(0001)¹ and VO_x monolayers on Rh(111)² (Fig. S2a). The V 2p intensity required fitting with two sets of doublets for the 2p^{1/2} and 2p^{3/2} contributions. The determined peak positions at 516 and 517.7 eV for V 2p^{3/2} indicate V ions in a very high oxidation state. For comparison, the corresponding peak maximum for bulk V₂O₃ (V³⁺) is at 515.5 eV, but shift to 515.2 and 516.1 eV for the $\sqrt{13}$ and $\sqrt{7}$ VO_x reconstruction on Rh(111), both with V ions in a formal 5+ oxidation state. The even higher binding energy detected here thus corroborates the V⁵⁺ oxidation state revealed from our DFT calculations. The presence of two peak maxima suggests the co-existence of two vanadium oxide phases on Ru(0001), a main one assigned to the mixed honeycomb oxide and a minority phase represented by the binary $\sqrt{48}$ VO_x oxide on Ru(0001).³ As the latter contains a substantial number of vanadyl V=O groups, the V 2p peaks shift to even higher energy here.

Also, the Fe 2p peaks required fitting with a minimum of two doublets. We abstain from a careful peak analysis here and have only added the literature values for Fe²⁺ and Fe³⁺ ions as a reference to the spectrum.⁴ Note that also the associated satellite positions have not been included for the sake of clarity. Evidently, the Fe 2p core level spectrum is compatible with the presence of Fe²⁺ and Fe³⁺ ions at the surface, with the former arising from the FeO(111) binary oxide and the latter from the mixed V/Fe honeycomb oxide film.

An intensity analysis of the V 2p and Fe 2p peaks, weighted by their respective sensitive factors, yields a mean V/Fe ratio of one to one, in agreement with the proposed stoichiometry of the mixed honeycomb film. This evaluation is necessarily subject to some uncertainty, as minor contributions of the parent oxides FeO and $\sqrt{48}$ VO_x are present on the Ru(0001) as well. As the mixed honeycomb phase clearly dominates on the surface, a significant deviation from a one-to-one cationic mixing ratio is not compatible with our spectra.

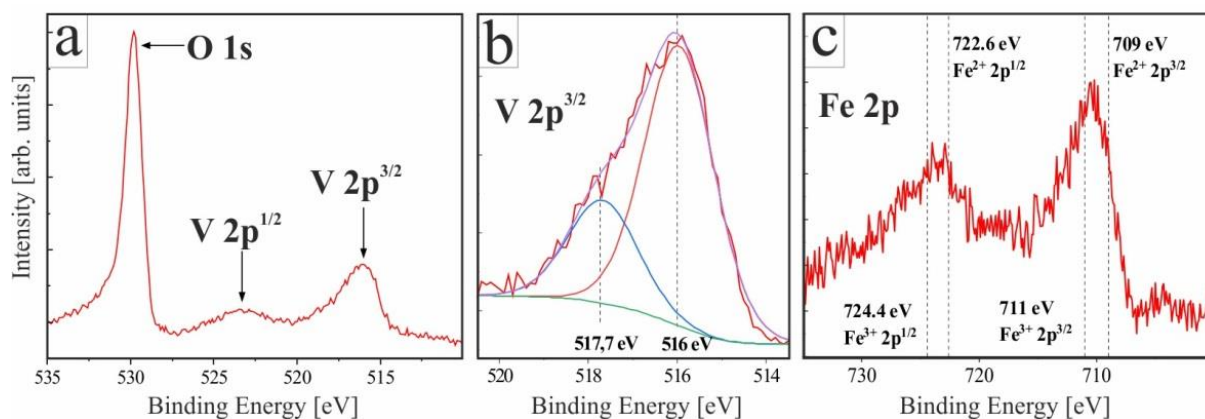


Figure S2: XP spectra measured for mixed V/Fe honeycomb films on Ru(0001) in the energy window of (a) the O 1s and V 2p and (c) the Fe 2p states. The vertical lines in (c) display the expected peak maxima for Fe²⁺ and Fe³⁺ contributions, taken from Ref. 4. Panel (b) shows a spectral deconvolution of the V 2p^{3/2} peak.

3. Atomic structures of VFeO_n films

Figure S3 represents top and side views of mixed films of VFeO_n composition deposited on the Ru(0001) substrate, as obtained by DFT optimization. Starting from the distorted honeycomb structure at n = 3 in which already one O-Ru bond per oxide formula unit is formed, there is a clear preference for additional oxygen atoms to be located at the interface to form bonds with both the cations of the oxide film and the surface Ru atoms.

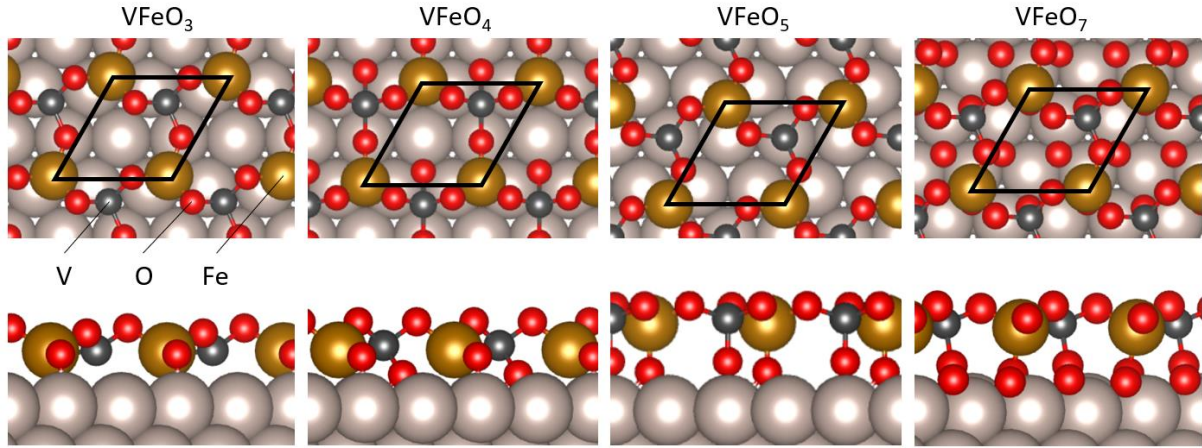


Figure S3: Top and side views of the most stable $VFeO_n$ films. Golden, red and grey balls represent Fe, O and V atoms, respectively. The (4×4)-Ru(0001) surface unit cell is indicated.

4. Electronic structure of $VFeO_6$ films

The electronic characteristics of mixed V/Fe oxide films on Ru(0001) were calculated using a DFT+U derived scheme as described in the main text. For the most stable $VFeO_6$ film, it is consistent with a large oxygen content. The local density of states (LDOS), Fig. S4, is characterized by the absence of nonbonding V 3d states below the Fermi level and a vanishing V magnetic moment, providing a clear signature of a vanadium 5+ formal oxidation state. Moreover, the Bader charge of V cations Q_V , Tab. S1, is very close to the corresponding value for the bulk V_2O_5 oxide ($Q_V = 2.10 e$). The LDOS of Fe atoms, as well as their charges and magnetic moments, preserve a character akin to Fe^{3+} in pure Fe_2O_3 ($Q_{Fe} = 1.74 e$; $\mu_{Fe} = 4.05 \mu_B$ in the bulk Fe_2O_3 oxide). The large cationic formal charges result from an electron transfer to the interfacial oxygen atoms O_A and O_B , the Bader charges of which are indeed close to those of the top-most oxygen atoms ($Q_{O_s} = -0.95 e$). In contrast, the charge of the oxygen atoms O_C are visibly smaller and close to those found for O atoms in the O(2×1)-Ru(0001) phase ($Q_O = -0.77 e$). As a result of the considerable oxygen content in the entire film, the Ru substrate becomes positively charged ($Q_{Ru} = 1.76 e/VFeO_6$), close to its charge found for the O(2×1)-Ru(0001) phase ($Q_{Ru} = 1.54 e/2O$). Considering the above cation oxidation states, the $VFeO_6$ film can be considered as a charge-neutral layer of $V^{5+}Fe^{3+}O^{-2}_4$ composition deposited on an O-covered Ru surface, with two such O atoms per $VFeO_4$ formula unit.

$Q_V (e), \mu_V (\mu_B)$	$Q_{Fe} (e), \mu_{Fe} (\mu_B)$	$Q_{O_A}, Q_{O_B}, Q_{O_C}, Q_{O_s} (e)$	$Q_{Ru} (e/VFeO_6)$
+2.07, 0.1	+1.69, 4.0	-0.90, -0.92, -0.79, -0.95	+1.76

Table S1. Electronic characteristics of the most stable $VFeO_6$ configuration: Bader charges Q and magnetic moments μ of the ions.

5. STM signatures of point defects in the $VFeO_6$ film

In support of Section 4.2 of the main text, Fig. S5 provides the simulated STM signatures of various types of defects in the $VFeO_6$ layer: V and Fe substitutions (sub) and interstitials (int), oxygen vacancies, and interfacial oxygen ad-atoms, all calculated for a (4×4)-Ru(0001) unit cell at +1.5 V sample bias.

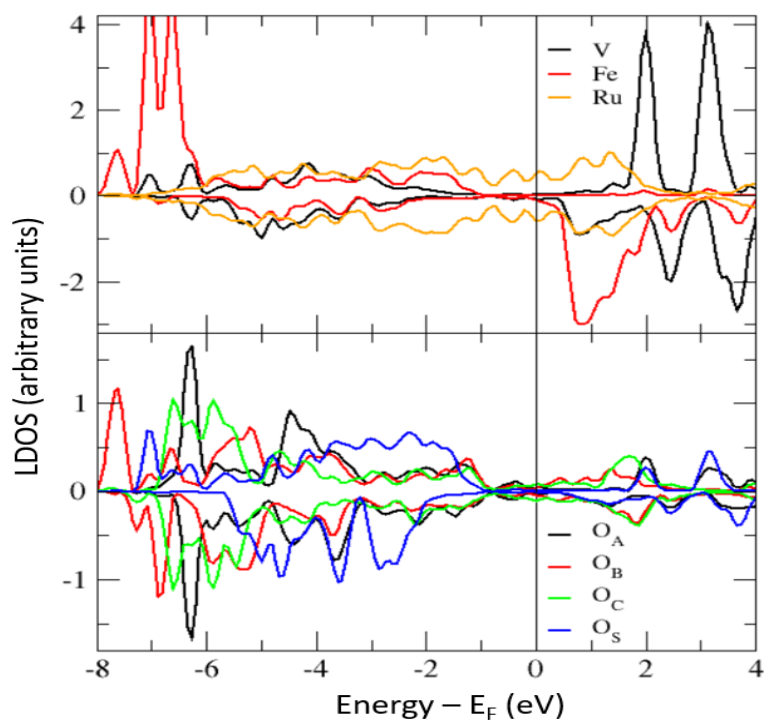


Figure S4. Projected densities of states of the Ru-supported VFeO_6 film: (top panel) Ru substrate and V, Fe cations, (bottom panel) different types of oxygen anions (O_A , O_B , O_C , and O_S).

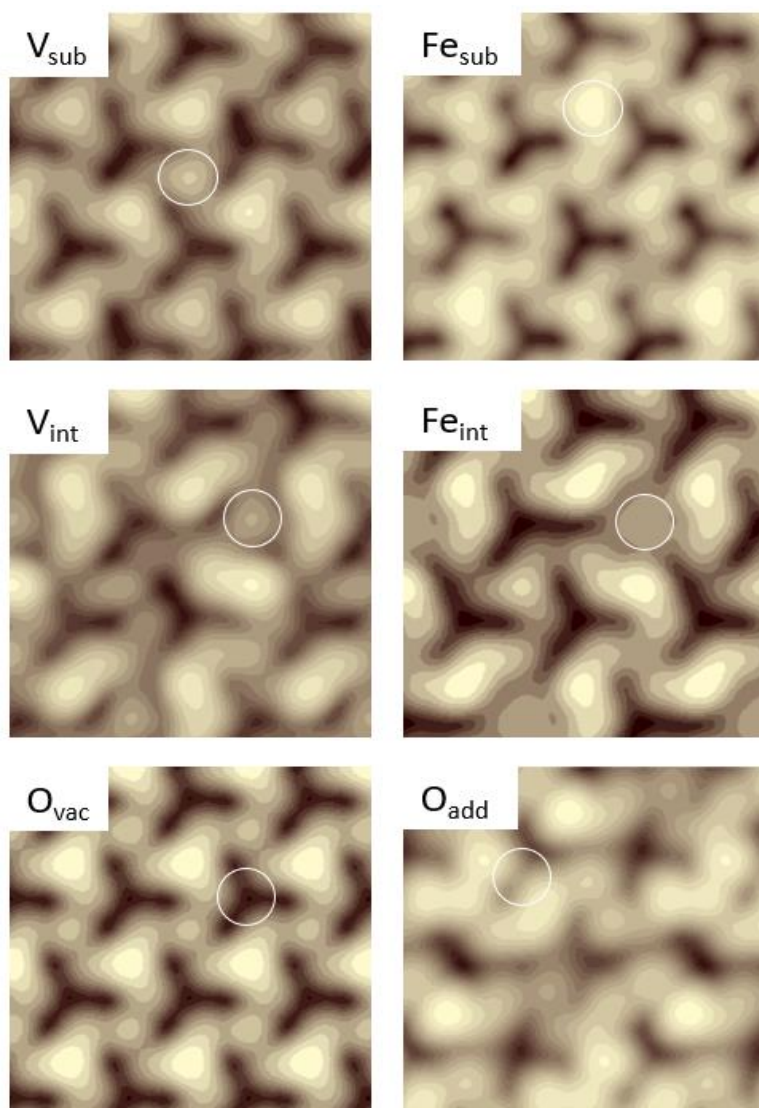


Figure S5. Simulated STM images of the VFeO_6 film at +1.5 V with point defects: V and Fe substitutions (sub), V and Fe interstitials (int), oxygen vacancy and adatom. Positions of the defects are indicated with white circles.

-
- ¹ Włodarczyk, R.; Sauer, J.; Yu, X.; Boscoboinik, J. A.; Yang, B.; Shaikhutdinov, S.; Freund, H. J. Atomic Structure of an Ultrathin Fe-Silicate Film Grown: A Monolayer of Clay? *J. Am. Chem. Soc.* **2013**, *135*, 19222–19228.
- ² Schoiswohl, J.; Sock, M.; Eck, S.; Surnev, S.; Ramsey, M. G.; Netzer, F. P.; Kresse, G. Atomic-Level Growth Study of Vanadium Oxide Nanostructures on Rh(111). *Phys. Rev. B - Condens. Matter Mater. Phys.* **2004**, *69*, 1–13.
- ³ Wang, Y.; Wemhoff, P. I.; Lewandowski, M.; Nilius, N. Electron stimulated desorption of vanadyl-groups from vanadium oxide thin films on Ru(0001) probed with STM, *Phys. Chem. Chem. Phys.* **2021**, *23*, 8439–8445.
- ⁴ Yamashita, T.; Hayes, P. Analysis of XPS spectra of Fe²⁺ and Fe³⁺ ions in oxide materials, *Appl. Surf. Sci.* **2008**, *254*, 2441–2449.